DL/SCI/P821E

preprint Daresbury Laboratory

AD-A255 710

DL/SCI/P821E

THE Ba-RELATED PARTIAL DENSITY OF STATES IN THERMIONIC DISPENSER CATHODES REVEALED BY RESONANT PHOTOEMISSION SPECTROSCOPY

by

A.M. AWOBODE, B.C.C. COWIE and D. NORMAN,
SERC Daresbury Laboratory.

DTIC
ELECTE
SEP 14 1992
S B D

Final Report to USAF (Grant AFOSR-89-0545).

92-25024

AUGUST, 1992

92 9 10 071

396 088 420528 9pp

Science and Engineering Research Council
DARESBURY LABORATORY
Daresbury, Warrington WA4 4AD

DISTRIBUTION STATEMENT A
Approved for public release;
Distribution Unlimited

REPORT DOCUMENTATION PAGE

Form Approved
OMB No. 0704-0188

Public reporting burden for this collection of information is estimated to average 1 hour per response, including the time for reviewing instructions, searching existing data sources, gathering and maintaining the data needed, and completing and reviewing the collection of information. Send comments regarding this burden estimate or any other aspect of this collection of information, including suggestions for reducing this burden, to Washington Headquarters Services, Directorate for Information Operations and Reports, 1215 Jefferson Davis Highway, Suite 1204, Arlington, VA 22202-4302, and to the Office of Management and Budget, Paperwork Reduction Project (0704-0188), Washington, DC 20503.

1. AGENCY USE ONLY (Leave blank)	2. REPORT DATE	3. REPORT TYPE AND DATES COVERED
	1992	Final 1 Sept 89 - 31 Aug 91

4. TITLE AND SUBTITLE

~~The surface structure of thermionic cathodes~~

See Cover

5. FUNDING NUMBERS

G AFOSR-89-0545

6. AUTHOR(S)

D Norman

7. PERFORMING ORGANIZATION NAME(S) AND ADDRESS(ES)

SERC Daresbury Laboratory
Warrington
Cheshire
WA4 4AD UK

8. PERFORMING ORGANIZATION REPORT NUMBER

DL/SCI/P821E

9. SPONSORING/MONITORING AGENCY NAME(S) AND ADDRESS(ES)

Department of the Air Force
European Office of Aerospace Research and Development
223/231 Old Marylebone Road
London NW1 5TH

10. SPONSORING/MONITORING AGENCY REPORT NUMBER

11. SUPPLEMENTARY NOTES

12a. DISTRIBUTION/AVAILABILITY STATEMENT

Unlimited

12b. DISTRIBUTION CODE

13. ABSTRACT (Maximum 200 words)

A range of synchrotron radiation-based spectroscopies has been used to study the geometric and electronic structure of the sub-monolayer barium/oxygen coating on tungsten-based thermionic dispenser cathodes. Surface EXAFS (Extended X-ray Absorption Fine Structure) results are identical to those published by us earlier (Norman et al, Phys. Rev. Lett. 58 (1987) 519). Near edge XAFS shows substantial differences between the environment of oxygen atoms on B-type (pure W matrix) and CD-type (W/Os alloy) cathodes, but these results still await detailed understanding. Photoemission shows that the shape of the valence band also is distinctly different for the two types of cathode, consistent with a lower coverage BaO overlayer on the alloy cathode, and a somewhat higher coverage of BaO with excess oxygen on the B-type cathode. The binding energies of the Ba $5p_{3/2, 1/2}$ and O 2s levels reinforce this suggestion. Constant initial state spectra show a resonance at a photon energy of about 106 eV in the Ba 5p levels and in parts of the valence band lying atbinding energies greater than ca. 3.5 eV, but there are no Ba-derived states within ca. 3.5 EV of the Fermi level.

14. SUBJECT TERMS

Thermionic cathodes; surface structure; photoemission; X-ray absoprtion spectroscopy.

15. NUMBER OF PAGES

13

16. PRICE CODE

17. SECURITY CLASSIFICATION OF REPORT	18. SECURITY CLASSIFICATION OF THIS PAGE	19. SECURITY CLASSIFICATION OF ABSTRACT	20. LIMITATION OF ABSTRACT
Unclassified	Unclassified	Unclassified	UL

THE Ba-RELATED PARTIAL DENSITY OF STATES IN THERMIONIC DISPENSER CATHODES REVEALED BY RESONANT PHOTOEMISSION SPECTROSCOPY

A.M. AWOBODE, B.C.C. COWIE and D. NORMAN

Science and Engineering Research Council, Daresbury Laboratory, Warrington WA4 4AD, UK

Photoemission excited by synchrotron radiation has been used to study the sub-monolayer barium/ oxygen coating on tungsten-based thermionic dispenser cathodes. The shape of the valence band is distinctly different for B-type (pure W matrix) and CD-type (W/Os alloy) cathodes. Comparison with published spectra for Ba and BaO facilitates the assignment of features consistent with a lower coverage BaO overlayer on the alloy cathode, and a somewhat higher coverage of BaO with excess oxygen on the B-type cathode. The binding energies of the Ba $5p_{\frac{1}{2},\frac{3}{2}}$ and O 2s levels reinforce this suggestion. Constant initial state spectra show a resonance at a photon energy of about 106 eV in the Ba 5p semi-core levels and in parts of the valence band lying at binding energies greater than ca. 3.5 eV, but there are no Ba-derived states within ca. 3.5 eV of the Fermi level. The resonance is broader for the valence band states than for the Ba 5p levels, as expected for their more extended wavefunctions, but we find no consistent difference between the two types of cathode.

DTIC QUALITY INSPECTED 3

Accession For	
NTIS GRA&I	☑
DTIC TAB	☐
Unannounced	☐
Justification	
By	
Distribution/	
Availability Codes	
Dist	Avail and/or Special
A-1	

1. Introduction

Thermionic dispenser cathodes are dominated by their surface properties, with a sub-monolayer coating maintaining a low work function and emitting high current densities for many years of operation [1]. They are made of polycrystalline tungsten substrates, impregnated with a mixture of oxides of calcium, aluminium and barium. In their operating temperature range of 1100 to 1400 K, the impregnant dissociates and a mixture of Ba and BaO diffuses through the pores between the tungsten crystallites and across the surface. This forms a submonolayer Ba-O-metal complex [2] in dynamic equilibrium with the Ba-containing evaporants being thermally desorbed from the surface. The work function (φ) is reduced to a value typically around 2 eV compared to the 4.5 eV of the pure tungsten. The performance of dispenser cathodes has been improved by coating the surface with third-row transition metal alloys or their alloys with tungsten. One of the best such metals is Os, reducing φ by a further 0.2 eV [3]. According to the Richardson–Dushman equation ($J \propto T^2 exp(-\varphi/T)$) this gives about a factor of ten increase in emitted current (J) at a given temperature T.

Cathodes have evolved semi-empirically to become highly efficient devices, although—despite much effort—the physics underlying their operation is still not fully understood. They have been probed by almost all of the tools of modern surface science [4] in attempts to determine what are the important atoms affecting the emitting properties and how they are arranged geometrically and electronically. Auger electron spectroscopy (AES) shows that the surface components are a monolayer or partial monolayer of barium on slightly oxidised tungsten [5], although the extent of bonding of barium and oxygen is debatable [1].

There has been little work on the electronic structure of cathode surfaces, most of the information being obtained indirectly from features such as interatomic Auger transitions [6]. Previous X-ray photoemission spectroscopy (XPS) studies have concentrated on analysis of the positions and line shapes of core levels and not studied the valence bands that are most affected by bonding [7,8]. One set of work using synchrotron radiation photoemission spectroscopy has been published [9,10], in which measurements of a type S cathode (pure W substrate) and a type M cathode were compared with spectra from Ba and BaO. The valence band of the type S cathode was found to be broader and more complex than that of the Os-Ru alloy-coated type M cathode [10]. Unfortunately some of this work suffers because the cathodes were not activated fully and the results thus cannot be

taken as representative of the surface of real cathodes. It is likely that significant amounts of the bulk oxide impregnant were present at the surface, and that the surface structure had not stabilised.

Some studies have looked at single crystal analogues of cathodes. Mueller et al [11] evaporated increasing thicknesses of stoichiometric BaO epitaxially onto a clean W(110) substrate. At low coverage, the photoelectron energy distribution curves (EDCs) show valence band features attributable to the BaO lying 6.4 and 4.2 eV below the Fermi level E_F. At higher coverages the spectra become dominated by a single peak at a binding energy of 4.6 eV, the same as in bulk BaO. Coincident with the development of this peak is a shift in binding energy of the O 2s level from 22.0 to 21.1 eV, also the same as bulk BaO. BaO adsorption on W(100) induces a prominent feature in the valence band 5.9 eV below E_F, not quite as large as the binding energy of 6.4 eV for p(2×1)O on the same surface [12].

Idealised analogues of cathodes have also been modelled theoretically. Using the full-potential linearised augmented plane wave (FLAPW) method Hemstreet et al [13,14] found that a c(2×2) BaO epitaxial layer on W(001) forms bonds between the d-like surface states of the tungsten substrate and both the Ba d and the oxygen 2p adsorbate levels. All possible combinations of interaction between adsorbate and substrate atoms are present. The main density of barium states lies within ca. 1 eV of E_F and the O 2p level peaks at ca. 4.2 eV, depending on the geometrical model assumed for the overlayer. Müller [15,16] used the relativistic $X\alpha$ method with Ba-O-W clusters of various sizes and also found complex bonding, with barium strongly oxidised while tungsten and oxygen were in a reduced chemical state. The presence of O enhances the charge transfer from Ba into the W substrate, leading to the lowered work function. The O 2p levels, however, are predicted to lie about 8.2 eV below E_F, in poor agreement with the experimental results [11,12].

Thus, there is a need for measurements of the density of states of well characterised cathode surfaces. In this work we have used photoemission to determine the electronic structure of samples of B-type cathodes, made from a pure W substrate, and CD-type cathodes, with a W-Os alloy surface. The variable photon energy from our synchrotron radiation source permits measurements on the shallow core levels as well, but more importantly allows separation of the barium-related partial density of the valence states.

2. Experimental procedure

The experiments were performed on beamline 6.1 at the Daresbury Synchrotron Radiation Source. Cathodes were obtained from Thorn-EMI-Varian Ltd, having been chosen to be representative of typical commercial cathodes. One B-type and two CD-type cathodes were mounted simultaneously on the manipulator such that each could be moved in turn into the photon beam. After bakeout of the experimental chamber the cathodes were heated to ca. 600°C for 23 h, followed by 11 h at 955°C, to remove any memory of their exposure to air. Each cathode was regenerated by heating to a temperature between 950° and 1050°C for 15 min to form a clean emitting surface approximately every 6 h during its measurement period, then allowed to cool for 15 min and measurements carried out at room temperature. The pressure was maintained below 1×10^{-10} mbar throughout the course of the experiments.

Photons in the energy range 70-170 eV were selected by a plane grating monochromator [17]. The photon flux incident on the sample varies as a function of photon energy because of the characteristics of the monochromator and the decay with time of the storage beam current. In the presentation of the data we have not corrected for these effects, but they are the same for all measurements and do not affect comparisons between spectra from different cathodes. The photon beam was incident on the cathode at 35° from the sample normal and photoelectron spectra were collected using a commercial (PHI) double pass cylindrical mirror analyser operated in fixed transmission mode and positioned in the horizontal plane at 90° to the incident beam. There are three components to the experimental resolution ΔE: the natural width of a feature, the bandwidth of the electron energy analyser and the bandwidth of the photon monochromator. ΔE has been measured in other experiments on this beamline [18] by fitting the Fermi-edge of a spectrum to a Fermi-Dirac distribution convolved with a Gaussian of width ΔE. Our resolution is dominated by the bandwidth of the photon monochromator and was found to increase with photon energy from 0.7 eV at $h\nu$=70 eV to 1.8 eV at $h\nu$=170 eV.

Two types of photoemission experiment were performed, (i) EDC spectra using a fixed photon energy, with the energy of the emitted electrons scanned and (ii) constant initial state (CIS) scans, with the electron kinetic energy scanned synchronously with the photon energy to keep a constant energy difference. In this mode one is probing transitions from the same initial state to a range of

final states varying with the photon energy. CIS scans were performed with the monochromator exit slits at a fixed setting so that the *wavelength* resolution was constant, but the *photon energy* resolution varies with $(h\nu)^2$ across the spectrum, but in the same way for all CIS spectra.

3. Results

Experimental EDC spectra at $h\nu$=100 eV, normalised to the peak intensity of the valence band, are given in Fig. 1 for the two different cathodes. The alloy cathode shows an almost constant density of states extending from the Fermi level to a binding energy of 3.2 eV, by comparison with which the pure tungsten cathode shows a reduced density of states near E_F with a peak about 2.3 eV below E_F. The spectrum from the CD-type cathode peaks at a binding energy of about 5.1 eV, with a well-resolved smaller peak at a binding energy of 7.4 eV. The B-type cathode shows a broader main peak, with its maximum at about 5.5 eV.

There were some changes in the EDCs with varying photon energy, which are best illustrated by the CIS spectra of Fig. 2 for the alloy (CD-type) cathode. The photoemitted intensity of the Ba 5p levels (Fig. 2(a)) peaks sharply as a function of photon energy at $h\nu$=106 eV and 120 eV. The intensity of the lower-lying valence band features (b) and (c) shows a broad increase with photon energy in the same range as that of (a), although extending to lower and higher energies than seen for (a). For feature (d), the valence band states 2.0 eV below the Fermi level, there is no such resonant enhancement. Similar results are obtained for the pure tungsten (B-type) cathode. For both types of cathode, the valence band resonance shows a lower energy onset and a greater breadth than for the Ba 5p core levels. We observe some small differences in the CIS spectra of the valence band features between B- and CD-type cathodes, but the differences observed are not consistent between our different samples and we plan further study of these phenomena.

The binding energies of all the shallow core levels were measured and are tabulated, along with the main features in the valence band, in Table 1.

4. Discussion

The resonance for the Ba 5p levels (Fig. 2(a)) occurs when the photon energy is greater than the binding energy of the Ba 4d levels, and is caused by a quasi

atomic excitation of the type

$$4d^{10}5s^25p^66s^2 \longrightarrow 4d^95s^25p^66s^24f^1 \longrightarrow 4d^{10}5s^25p^56s^2 + e^- \qquad (1)$$

with a final state, closely resembling a 4f wavefunction inside the potential barrier [19], which decays non-radiatively into the direct 5p photoemission channel, thus increasing its intensity. Electrons excited from the Ba 4d states are expected to be highly localised on the Ba atoms, and the well defined resonance indicative of a long-lived 4f intermediate state is confirmation of this point. The Ba 5p resonance is largely an atomic effect and is not helpful in deducing details of cathode physics and chemistry.

On the other hand, the valence band states resonate much more weakly *via a mechanism of the type*

$$4d^{10}5s^25p^66s^2 \longrightarrow 4d^95s^25p^66s^24f^1 \longrightarrow 4d^{10}5s^25p^66s^1 + e^- \qquad (2)$$

As with the 5p levels, this process depends on localisation of the excited electron on a Ba atom, and the occurrence and strength of a resonance can be used as a measure of the spatial origin of the electron states probed. In other words, the key to this effect is the overlap of wavefunctions between Ba 4d and Ba 5p (localised, core) and Ba 6s valence (extended) states. The CIS spectra of the two main peaks of the valence band (Figs. 2(b) and (c)) resonate with the Ba 4d levels and thus we can deduce that these states are Ba-related. The CIS spectrum of Fig. 2(d) *does not show a resonance, therefore there is no Ba character in the states within* ca. 3.5 eV of the Fermi level. These are the key findings of this work.

We note that the binding energy of the Ba 4d core levels is about 90 eV but the resonance in the 5p levels occurs a little above this energy, peaking at $h\nu$=106 eV. This is a well-known phenomenon [19] caused by the high angular momentum (l = 3) of the outgoing 4f photoelectron wave giving a centrifugal barrier in the potential, leading to 'delayed onset.' There is some evidence in Fig. 2(a) for the sharp peak at 94.3 eV seen in all Ba compounds and attributed to $4d^94f^1\ ^3P$ final states, but the photon energy increment in our measurements was set too coarsely to resolve this feature fully.

A discrete peak at about 120 eV is also seen in the CIS spectrum for the Ba 5p levels. This peak is not due to the splitting between the $5p_{\frac{3}{2}}$ and $5p_{\frac{1}{2}}$ core levels, which is only 1.8 eV. CIS spectra taken at energy differences of 14.6, 16.4 and 15.5 eV, (corresponding to the $5p_{\frac{3}{2}}$ peak, the $5p_{\frac{1}{2}}$ peak and half-way in

between), all show the same structure of CIS, with a well separated second peak at $h\nu$=120 eV. This peak is also seen in the photoabsorption spectra of pure Ba, Ba^{+} and Ba^{++} [20] and in compounds such as $BaBr_2$, $BaCl_2$ and BaF_2 [21]. It has been suggested as being due to a two-hole final state involving a 4d and a 5p hole,

$$4d^{10}5s^25p^66s^2 \longrightarrow 4d^95s^25p^56s^2nln'l' \qquad (3)$$

where $nln'l'$ is postulated to be $(5d5d)$ [22] although other configurations such as $(6p4f)$ are also allowed, and the full understanding of this feature is still awaited. Similar Ba resonances are seen in the $YBa_2Cu_3O_{7-\delta}$ high-T_C superconductors [23,24,25,26,27,28] and in $Ba_{0.6}K_{0.4}BiO_3$ [29]. However, there is no clear evidence for this 120 eV peak in our valence band CIS spectra (Fig. 2(b) and (c)), perhaps suggesting that its existence is related to the hybridisation of energy levels.

The Ba-related contribution to the valence band has also been deduced in a different way from experiments involving deposition of increasing thicknesses of epitaxial overlayer of BaO on W(110) [11]. Initially, at low coverage, features are found at binding energies of 4.2 and 6.4 eV. The peaks at 5.3 and 7.4 eV for our CD-type cathode probably correspond to these peaks for sub-monolayer BaO. At higher coverages, around a monolayer, a peak develops at 4.6 eV below E_F, the same energy as the main valence band peak in bulk BaO [12]. This is similar to our result for the B-type cathode, where the spectrum is dominated by a single peak.This suggests that the surface of B-type cathodes is more similar to bulk BaO than CD-type cathodes are, and fits the expectation from the higher coverage data of [12]. Previous work [30] also found less BaO adsorbate material on a CD cathode. This could be explicable by the observation, especially on immature B-type cathodes, of pore ends contributing up to 20% of the surface Ba; these are covered up on alloy cathodes. Our finding of a somewhat lower binding energy for the O 2s level on B-type than CD-type cathodes is also consistent with a higher concentration of BaO on B-type samples.

There is known to be excess O on cathode surfaces [31]—particularly on B-type—but this is O not interacting with Ba/O [32,33]. Extra O with BaO on W(001) has been reported to give higher DOS 2-3.5 eV below E_F [12]: this probably explains the extra intensity in the valence band peaking at 2.2 eV in our B-type spectra, and also the second O 2s peak on B-type probably corresponds to oxygen in different bonding states.

The finding that there is no Ba character in the states near to the Fermi level contrasts strongly with the predictions of the FLAPW calculations [14], although we note that a photoemission spectrum will not necessarily look the same as the density of states (DOS) because of the selection rules and matrix elements for the photoemission process. Neither do we see the large peak centred 0.85 eV below Fermi level found in these calculations [14]. Although working cathodes are complicated compared to the simplified W(001) surface calculated, there is good experimental evidence that they mimic real cathodes quite successfully, and we have no explanation for the major discrepancies found here.

5. Conclusion

Photoemission has been used to study the partial density of states in different types of thermionic dispenser cathode. Resonance effects arising from excitation of the Ba 4d core levels have been used to identify the Ba-related part of the valence band. There are no Ba states within ca. 4 eV of the Fermi level, and all the Ba weight lies in a region peaking about 5.5 eV below E_F.

Acknowledgments

This work was supported in part by USAF Grant AFOSR-89-0545. The SERC is acknowledged for the award of beamtime at the SRS. We are very grateful to R.A. Tuck and H.B. Skinner of Thorn-EMI-Varian Ltd for supplying cathodes and for fruitful discussions. We appreciate helpful discussions with J.A.D. Matthew on the nature of photoemission resonances.

References

1 R.A. Tuck, Vacuum 33 (1983) 715.
2 R. Forman, Appl. Surface Sci. 2 (1979) 258.
3 M.C. Green, H.B. Skinner and R.A. Tuck, Appl. Surface Sci. 8 (1981) 13.
4 see, for instance, the proceedings of the series of Tri-Service Cathode Workshops published in Appl. Surface Sci. 2 (1979); 8 (1981); 16 (1983) and 24 (1985).
5 R. Forman, J. Appl. Phys. 47 (1976) 5272.

6 G.A. Haas, A. Shih and C.R.K. Marrian, Appl. Surface Sci. 16 (1983) 139.
7 D. Jones, D. McNeely and L.W. Swanson, Appl. Surface Sci. 2 (1979) 232.
8 W.V. Lampert, K.D. Rachocki, B.C. Lamartine and T.W. Haas, J. Electron Spectrosc. and Relat. Phenom. 26 (1982) 133.
9 D.S. Chen, I. Lindau, M.H. Hecht, A.J. Viescas, J. Nogami and W.E. Spicer, Appl. Surface Sci. 13 (1982) 321.
10 M.H. Hecht, I. Lindau and D.S. Chen, J. Appl. Phys. 53 (1982) 9021.
11 D.R. Mueller, R.L. Kurtz, R.L. Stockbauer, T.E. Madey and A. Shih, Surface Sci. 237 (1990) 72.
12 D. Mueller, A. Shih, E. Roman, T. Madey, R. Kurtz and R. Stockbauer, J. Vac. Sci. Technol. A6 (1988) 1067.
13 L.A. Hemstreet, S.R. Chubb and W.E. Pickett, J. Vac. Sci. Technol. A6 (1988) 1063.
14 L.A. Hemstreet, S.R. Chubb and W.E. Pickett, Phys. Rev. B 40 (1989) 3592.
15 W. Müller, J. Vac. Sci. Technol. A6 (1988) 1072.
16 W. Müller, IEEE Trans. Electron Devices 36 (1989) 180.
17 M.R. Howells, D. Norman, G.P. Williams and J.B. West, J. Phys. E: Sci. Instrum. 11 (1978) 199.
18 R.J. Cole, J.A. Evans, L. Duò, A.D. Laine, P.S. Fowles, P. Weightman, G. Mondio and D. Norman, Phys. Rev. B, in press.
19 J.-P. Connerade, Contemp. Phys. 19 (1976) 415.
20 T.B. Lucatorto, T.J. McIlrath, W.T. Hill III and C.W. Clark, in *X-Ray and Atomic Inner-Shell Physics* (American Institute of Physics, New York, 1982) p. 584.
21 P. Rabe, Ph. D. Thesis, University of Hamburg, DESY Interner Bereicht No. F41-74/2 (1974).
22 G. Wendin, in *VUV Radiation Physics*, ed. E.E. Koch *et al* (Vieweg-Pergamon, Berlin, 1974), p. 225.
23 R. Kurtz, R.L. Stockbauer, D. Mueller, A. Shih, L.E. Toth, M. Osofsky and S.A. Wolf, Phys. Rev. B 35 (1987) 8811.
24 M. Onellion, Y. Chang, D.W. Niles, R. Joynt, G. Margaritondo, N.G. Stoffel and J.M. Tarascon, Phys. Rev. B 36 (1987) 819.
25 Z. Shen, J.W. Allen, J.J. Yeh, J-S. Kang, W. Ellis, W. Spicer, I. Lindau, M.B. Maple, Y.D. Dalichaouch, M.S. Torikachvili, J.Z. Sun and T.H. Geballe, Phys. Rev. B 36 (1987) 8414.
26 T. Takahashi, F. Maeda, H. Arai, H. Katayama-Yoshida, Y. Okabe, T. Suzuki, S. Hosoya, A. Fujimori, T. Shidara, T. Koide, T. Miyahara, M. Onoda, S. Shamoto and M. Sato, Phys. Rev. B 36 (1987) 5686.
27 J.A. Yarmoff, D.R. Clarke, W. Drube, U.O. Karlsson, A. Taleb-Ibrahimi and F.J. Himpsel, Phys. Rev. B 36 (1987) 3967.
28 A.J. Lowe, D. Greig, M.A. Howson, M.J. Walker, H.H. Boghosian, R. Stevens, Y.L. Chen, D.S-L. Law, D. Norman, F.M. Quinn and J.A.D. Matthew, J. Phys. C: Solid State 21 (1988) L763.
29 M.W. Ruckman, D. Di Marzio, Y. Jeon, G. Liang, J. Chen, M. Croft and M.S. Hegde, Phys. Rev. B 39 (1989) 7359.
30 H.B. Skinner and R.A. Tuck, Final Report on Project RP5-37, UK Ministry of Defence (1982) (unpublished).
31 J. Hasker and H.J.H. Stoffelen, Appl. Surface Sci. 24 (1985) 330.
32 C.R.K. Marrian, A. Shih and G.A. Haas, Appl. Surface Sci. 16 (1983) 1.
33 G.A. Haas, A. Shih and C.R.K. Marrian, Appl. Surface Sci. 24 (1985) 430.

Figure Captions

Figure 1. Valence band photoelectron spectra, normalised to the intensity of the Fermi level, for a B-type and a CD-type cathode, taken at $h\nu$=100 eV.

Figure 2. Constant initial state spectra for the B-type cathode, measured for the initial state energies indicated on the energy distribution curve shown in the inset.

Table 1 Binding energies of shallow core levels and the main features in the valence bands for B-type and CD-type cathodes found in this work

	B-type	CD-type
valence band	2.2 ± 0.1	
	5.5 ± 0.1	5.3 ± 0.1
		7.4 ± 0.1
Ba $5p_{3/2}$	16.4 ± 0.2	16.0 ± 0.2
Ba $5p_{1/2}$	14.6 ± 0.2	14.3 ± 0.2
O 2s	22.0 ± 0.3	22.4 ± 0.3
	25.5 ± 0.6	
W $4f_{7/2}$	31.5 ± 0.2	31.6 ± 0.2
W $4f_{5/2}$	33.6 ± 0.2	33.7 ± 0.2
Os $4f_{7/2}$		49.9 ± 0.2
Os $4f_{5/2}$		52.7 ± 0.2

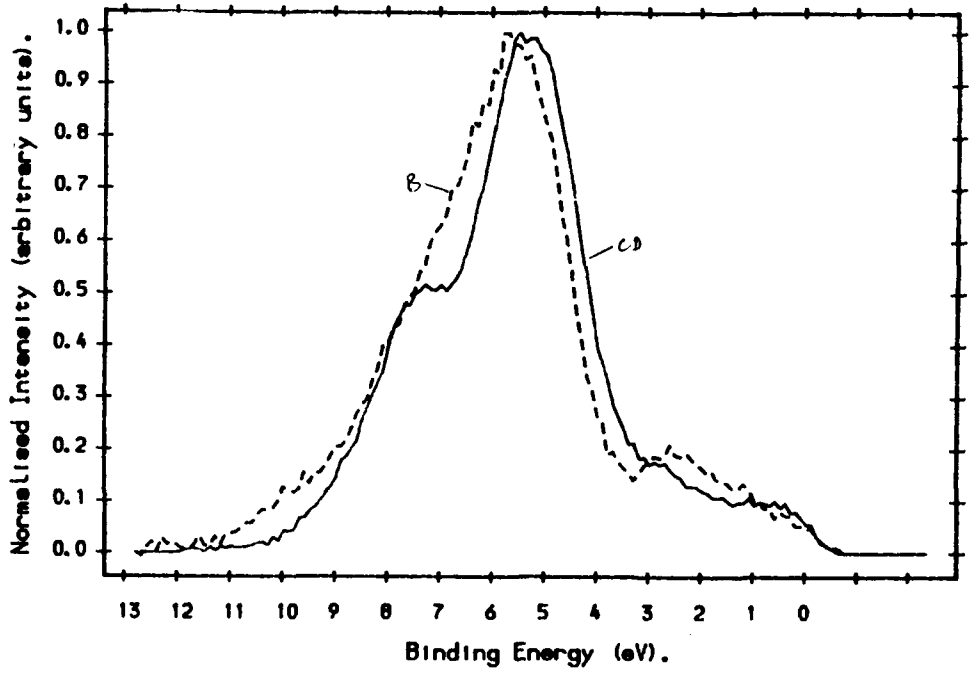

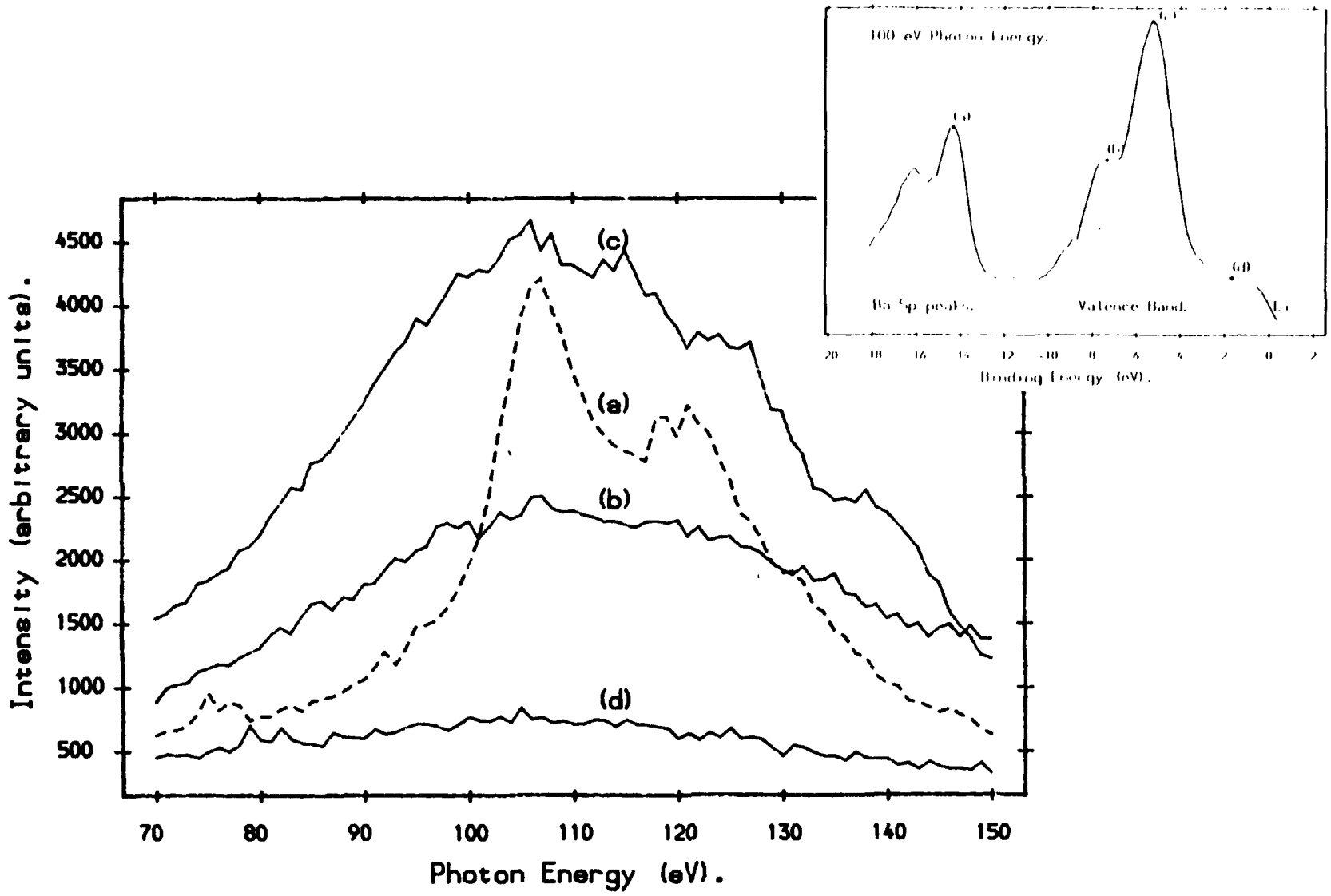
Intensity (arbitrary units).
4500
4000
3500
3000
2500
2000
1500
1000
500
70
80
90
100
110
120
130
140
150
Photon Energy (eV).
(c)
(a)
(b)
(d)
100 eV Photon Energy.
Ba 5p peaks.
Valence Band.
Binding Energy (eV).